are removed and burnt. The rather high temperature at which these phenomena occur shows that these organic groups are chemically bonded to the oxide network and not adsorbed only as solvent molecules. All organic ligands have not been removed by the substoichiometric hydrolysis (h = 1.9). The xerogel should then be described as an oxopolymer $Nb_2O_{5-x}(OR)_{2x}$ where OR correspond to both OAc and $OPent^n$ groups (Figure 3c). TGA shows that x is around 0.8, and NMR experiments suggest that the OAc/OPent ratio is close to 1/1. The powder remains amorphous up to 620 °C, where the exothermic peak corresponds to the crystallization of T-Nb_2O_5.[23] Actually X-ray diffraction experiments performed in a heating chamber show that crystallization occurs at lower temperatures, near 550 °C.

Conclusions

The synthesis of monolithic gels requires a careful control of the chemistry. Uncontrolled precipitation must be avoided. The synthesis of polymeric gels must be promoted.[30] Monolithic niobium pentoxide based gels can be reproducibly obtained when substoichiometric hydrolysis of niobium alkoxide precursors $Nb(OR)_5$ (OR = OPent) is performed in the presence of acetic acid. This carboxylic acid changes the alkoxide precursor at a molecular level and leads to new precursors $Nb(OPent)_{5-x}$-

$(OAc)_x$ (x = 0.1). They are mainly dimers and monomers with acetate ligands in both bridging and chelating positions. ^{93}Nb NMR experiments are in progress in order to provide a better identification of the different molecular precursors in the solution. The chemical control of hydrolysis and condensation reactions seems to be related to the role of acetate ligands, which are difficult to remove.[30,31] More precisely, as shown from IR measurements, chelating acetates are still present in the xerogel, suggesting that bridging carboxylates are preferentially removed over chelating ones. Monolithic transition-metal oxide gels are preferentially obtained with polymeric networks. Their formation is promoted by decreasing the functionality of the precursor. Condensation rates also have to be slowed down with respect to the hydrolysis rate.[30,31] As a consequence niobium oxide based gels synthesized in the presence of acetic acid probably have a polymeric nature. SAXS experiments should provide more information on the shape and morphology of such gels. The xerogel obtained after drying the gel at 80 °C is an oxopolymer containing organic groups chemically bonded to the oxide backbone. Upon heating in air at 500 °C pure tetragonal Nb_2O_5 powders have been obtained.

(30) Sanchez, C.; Livage, J. *New J. Chem.* **1990**, *14*, 513.

(31) Doeuff, S.; Henry, M.; Sanchez, C.; Livage, J. *J. Non-Cryst. Solids* **1987**, *89*, 206.

Dimensionally Stable MEEP-Based Polymer Electrolytes and Solid-State Lithium Batteries

K. M. Abraham* and M. Alamgir

EIC Laboratories, Inc., 111 Downey Street, Norwood, Massachusetts 02062

Several methods have been developed to dimensionally stabilize polymer electrolytes based on poly-[bis((methoxyethoxy)ethoxy)phosphazene] (MEEP). In contrast to the poor dimensional stability exhibited by complexes of MEEP with most Li salts, those prepared with $LiAlCl_4$ have been isolated as the first example of free-standing $MEEP-(LiX)_n$ films. The mechanical properties of dimensionally unstable $MEEP-(LiX)_n$ complexes can be significantly improved by forming composites with polymers such as poly(ethylene oxide), poly(propylene oxide), poly(ethylene glycol diacrylate) and poly(vinylpyrrolidinone). The conductivity of 6.7×10^{-5} Ω^{-1} cm^{-1} at 25 °C exhibited by 55 wt% MEEP/45 wt% $PEO-[LiN(CF_3SO_2)_2]_{0.13}$ is among the highest values reported to date for a dimensionally stable electrolyte. The preparation and conductivity, calorimetric, and electrochemical studies of these electrolytes are described. Cyclic voltammetric data indicated that they are anodically stable at least up to 4.5 V versus Li^+/Li. They have shown excellent compatibility with Li metal, making them suitable for use as Li^+ conductive solid electrolytes in solid-state Li batteries. Li/TiS_2 solid-state cells utilizing some of these electrolytes have exceeded 200 cycles.

Introduction

Li^+-conductive polymer electrolytes derived from Li salt complexes of poly[bis((methoxyethoxy)ethoxy)phosphazene] (MEEP), due to their high ambient temperature conductivity, are of considerable importance for the fabrication of solid-state Li batteries.[1-3] They have exhibited 3–4 orders of magnitude higher conductivity at room temperature than electrolytes based on their poly(ethylene oxide) (PEO) counterparts. However, the poor mechanical properties of MEEP-based electrolytes has presented

practical problems when attempts were made to fabricate all-solid-state Li batteries incorporating them.[2,4] At room temperature and above, these complexes are glutinous materials with a tendency to flow under pressure. Several

(1) Blonsky, P. M; Shriver, D. F.; Austin, P.; Allcock, H. R. *J. Am. Chem. Soc.* **1984**, *106*, 6854.

(2) Abraham, K. M.; Alamgir, M.; Perrotti, S. J. *J. Electrochem. Soc.* **1988**, *135*, 535.

(3) Semkow, K. W.; Sammels, A. F. *J. Electrochem. Soc.* **1987**, *134*, 766.

(4) Alamgir, M.; Reynolds, R. K.; Abraham, K. M. In *Proceedings of the Symposium on Materials and Processes for Li Batteries*; Abraham, K. M., Owens, B. B., Eds.; The Electrochemical Society: Pennington, NJ, 1989; PV89-4, p 321.

*To whom correspondence should be addressed.

approaches have been pursued to enhance the mechanical properties of MEEP. These include chemical cross-linking of MEEP with poly(ethylene glycol)[5] irradiation of MEEP or MEEP-(LiX)$_{0.25}$ complexes with various doses of ^{60}Co γ-ray to induce cross-linking,[6,7] and the use of porous, fiberglass support matrix.[4]

We have found[2,4,8,9] that the dimensional stability of MEEP-(LiX)$_n$ complexes can be improved to prepare free-standing films by forming composites with high molecular weight PEO or poly(propylene oxide) (PPO). Films were cast from solutions containing requisite amounts of MEEP, PEO, or PPO and a Li salt in acetonitrile. We have now extended the class of dimensionally stable MEEP-based composite polymer electrolytes to include blends of MEEP with in situ photopolymerized poly(ethylene glycol diacrylate) (PEGDA) and poly(vinylpyrrolidinone) (PVP). Composite electrolytes formed between MEEP-(LiX)$_n$ and each of them have shown electrical and mechanical characteristics similar to those containing the poly(olefin oxide)s, PEO and PPO.

We have also discovered that complexes of MEEP and LiAlCl$_4$ can be isolated as dimensionally stable electrolytes. To our knowledge, this is the first example of a MEEP-(LiX)$_n$ electrolyte that can be processed into free-standing, thin films without such physical treatment as γ-radiation or the addition of a mechanically strong second polymer. Not only are the LiAlCl$_4$ complexes mechanically stable, but they also possess conductivities very close to those of other MEEP-(LiX)$_n$ electrolytes.

The electrical, thermal, and structural properties of these various dimensionally stable electrolytes we have prepared are reported here. While the emphasis in this paper is on MEEP-(LiAlCl$_4$)$_n$ and the composite electrolytes formed with PVP and PEGDA, some of the results for MEEP/PEO-(LiX)$_n$ and MEEP/PPO-(LiX)$_n$ composites are included to put the structural properties and electrical behavior of the general family of dimensionally stable MEEP-based electrolytes into perspective. In addition, solid-state Li/TiS$_2$ cells using a selected group of these electrolytes have been constructed and electrochemically cycled at different temperatures and rates.

Experimental Section

MEEP was synthesized according to the procedure of Allcock et al.[10] The details of our preparation have been reported earlier.[8]

PEO (Polysciences) of average molecular weight 5×10^6 was used as received after drying under vacuum at 50 °C. LiClO$_4$, LiBF$_4$, and LiN(CF$_3$SO$_2$)$_2$ were dried under vacuum at temperatures around 120 °C. LiAlCl$_4$ obtained from Anderson Physics was used as received. Tetraethylene glycol diacrylate (Aldrich), the precursor for PEGDA films, was purified by passing it through an inhibitor remover column. Vinylpyrrolidinone (Aldrich) was purified by distilling under vacuum.

Pure MEEP-(LiAlCl$_4$)$_n$ electrolytes were prepared by dissolving MEEP and the corresponding amount of LiAlCl$_4$ in acetonitrile. The mixture was then homogenized by stirring in order to prepare bubble-free electrolyte films. The films, cast by pouring the solution onto Teflon dishes, were allowed to dry at room temperature inside an argon-filled glovebox. Subsequently, they were dried under vacuum (<0.1 Torr) at 45–50 °C for 2 days. The dried films, the thickness of which varied between 4 and 6 mils, were

stored in the glovebox. The preparation of the composite electrolytes was carried out in two different ways. For the MEEP/PEO-(LiX)$_n$ and MEEP/PPO-(LiX)$_n$ electrolytes, appropriate amounts of PEO or PPO, MEEP, and a Li salt were dissolved together in acetonitrile and cast into thin films as described above. Dimensional stabilization of MEEP electrolytes by reinforcement with PVP or PEGDA was carried out in the following manner: A known quantity of vinylpyrrolidinone or tetraethylene glycol diacrylate in conjunction with a few drops of a photoinitiator was added to a solution of MEEP-(LiClO$_4$)$_{0.25}$ in acetonitrile. After evaporation of acetonitrile at room temperature, the mixture was irradiated with UV light (λ = 365 nm) for about 5 min, which resulted in the formation of mechanically stable films. They were again dried at 45–50 °C under vacuum for 2 days.

The electrochemical behavior of neat MEEP-(LiClO$_4$)$_{0.25}$ electrolytes was studied after stabilizing them in a separator matrix.[4] It was accomplished by spreading the electrolyte on a 2-mil-thick fiberglass separator paper and wetting it with a few drops of tetrahydrofuran until the electrolyte was homogeneously distributed within the porous matrix. The solvent was then pumped off.

Characterization of the polymer electrolytes was carried out using complex impedance spectroscopy, differential scanning calorimetry (DSC), cyclic voltammetry, X-ray diffraction, and infrared spectroscopy. The DSC data were obtained by using a Perkin-Elmer DSC7 calorimeter. Complex impedance measurements between 100 kHz and 5 Hz were performed using an EG&G PAR Model M378 impedance system and stainless steel electrodes.[8] X-ray diffraction patterns were obtained by using a Rigaku X-ray diffractometer and Cu K$_\alpha$ radiation. Infrared spectra were recorded on an IBM 9000 FTIR spectrometer with the electrolyte sandwiched between KBr windows.

Cyclic voltammetry on the polymer electrolytes was carried out at 75 °C on a stainless steel or a gold working electrode using Li both as the counter and reference electrodes. An EG&G PAR Model 175 universal programmer in conjunction with an ECO Model 551 potentiostat and a Bascom-Turner $X-Y$ recorder (Model 4110) was used to carry out the voltammetric experiments. The electrolyte was sandwiched between the working and the Li electrodes.

The transport number for Li$^+$ in the polymer electrolytes was determined by using the potentiostatic polarization technique in cells of the configuration Li/polymer electrolyte/Li.[11] A constant voltage of 25 mV was applied to the cell. The resulting current was monitored as a function of time with a recorder until a steady-state current was attained. The transport number, t_+, was calculated as the ratio between the values of the steady-state and initial currents.

Experimental Li/TiS$_2$ cells were constructed with the polymer electrolyte sandwiched between a 0.005-cm-thick Li foil anode pressed onto a Ni screen and a TiS$_2$ composite cathode. The TiS$_2$ electrodes were prepared by spreading a mixture of 80 wt% TiS$_2$, having a stoichiometric composition of Ti$_{1.02}$S$_2$ prepared in-house, and 20 wt% polymer electrolyte of the composition 70 MEEP/30 PEO-(LiX)$_{0.13}$ on one side of a Ni foil. All the cells were constructed in the cathode-limited configuration. The electrode package was secured between plastic plates with a positive pressure applied to the plates by means of compression springs to allow good interfacial contact between the electrodes. Cells were cycled between 3.0 and 1.6 V at constant currents and at several temperatures.

Results and Discussion

Several dimensionally stable, Li$^+$-conductive MEEP-based polymer electrolytes have now been prepared in our laboratories, allowing the utilization of these highly conductive electrolytes in all-solid-state rechargeable Li batteries that can be operated at ambient temperatures. The family of dimensionally stable electrolytes based on MEEP now includes the following: MEEP-(LiAlCl$_4$)$_n$ complexes;

(5) Tonge, J. S.; Shriver, D. F. *J. Electrochem. Soc.* **1987**, *134*, 269.

(6) Nazri, G.; MacArthur D. M.; Ogara, J. F. *Chem. Mater.* **1989**, *1*, 370.

(7) Bennet, J. L.; Dembek, A. A.; Allcock, H. R.; Heyen, B. J.; Shriver, D. F. *Chem. Mater.* **1989**, *1*, 4.

(8) Abraham, K. M.; Alamgir, M.; Reynolds, R. K. *J. Electrochem. Soc.* **1989**, *136*, 3576.

(9) Abraham, K. M.; Alamgir, M.; Moulton, R. D. *J. Electrochem. Soc.* **1991**, *138*, 921.
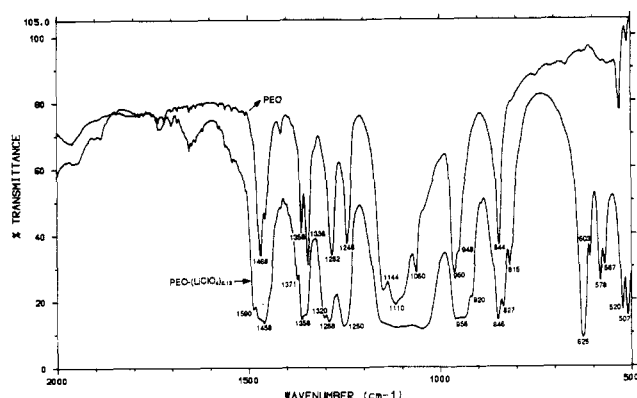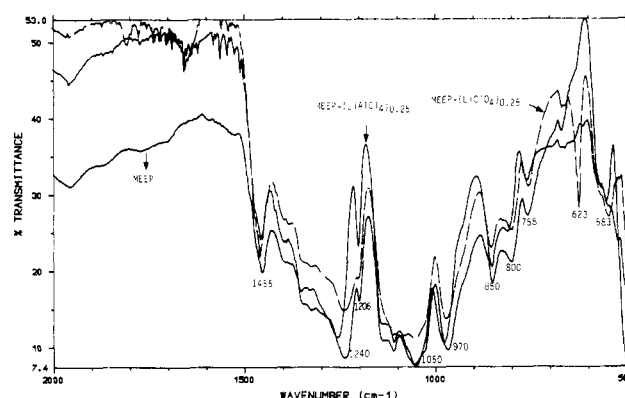
(10) Allcock, H. R.; Austin, P. E.; Neenan, T. X.; Sisko, J. T.; Blonsky, P. M.; Shriver, D. F. *Macromolecules* **1986**, *19*, 1508.

(11) Blonsky, P. M.; Shriver, D. F.; Austin, P.; Allcock, H. R. *Solid State Ionics* **1986**, *18/19*, 258.

MEEP-Based Polymer Electrolytes

Chem. Mater., Vol. 3, No. 2, 1991 341

Chart I

MEEP/PEGDA-(LiX)$_n$ or MEEP/PVP-(LiX)$_n$ electrolytes, where LiX include LiBF$_4$ and LiClO$_4$ obtained by in situ photopolymerization; MEEP/PEO-(LiX)$_n$ or MEEP/PPO-(LiX)$_n$ complexes, where LiX include LiBF$_4$, LiClO$_4$, LiAsF$_6$, LiCF$_3$SO$_3$, LiAlCl$_4$, and LiN(SO$_2$CF$_3$)$_2$; MEEP-(LiX)$_n$ supported on a porous matrix such as a fiberglass separator.

The structural formulas of the polymers employed in this study are given in Chart I and are useful for visualizing the structure–property relationships of the related electrolytes. While PVP is shown as a linear polymer, it is possible that a certain amount of cross-linking does occur in the photopolymerization process. The PEGDA is believed to be a predominantly cross-linked polymer.[12]

Explanations for formulas of the electrolytes described in this paper are as follows. In the single-polymer electrolytes, PEO-(LiX)$_n$, PPO-(LiX)$_n$, and MEEP-(LiX)$_n$, the subscript n is the Li$^+$ to O mole ratio wherein complexes of the stoichiometries (PEO)$_8$LiX, (PPO)$_8$LiX, and (MEEP)$_4$LiX are assumed to form. In the mixed polymer electrolytes the polymer ratios are given in weight percentages. The concentration of the Li salt in the MEEP/PEO and MEEP/PPO mixed electrolytes is selected in such a way that the Li$^+$ to O mole ratios are additive functions of those in the corresponding single-polymer electrolytes. In the MEEP/PVP and MEEP/PEGDA electrolytes only MEEP is assumed to complex with Li$^+$.

Physical Properties of MEEP-Based Electrolytes. MEEP and its Li salt complexes such as MEEP-(LiBF$_4$)$_{0.25}$, MEEP-(LiClO$_4$)$_{0.25}$, and MEEP-(LiSO$_3$CF$_3$)$_{0.25}$ are glutinous materials with a tendency to flow even under slight compression. Against this experience, it was surprising to find that MEEP doped with LiAlCl$_4$ could be processed into dimensionally stable, free-standing thin films. As mentioned earlier, this is the first example of a MEEP-(LiX)$_n$ complex that demonstrates such a property without the addition of a second polymer, immobilization in a support matrix, or the use of high-energy radiation to cross-link. Homogeneous and uniform films of complexes having various MEEP to LiAlCl$_4$ ratios have been prepared and studied. Thin films of these electrolytes appeared almost clear. These films were found to be highly sensitive to moist atmosphere. For example, a piece of film lost all its dimensional stability and became a liquid mass upon sitting in the normal atmosphere overnight.

MEEP-based electrolytes containing a reinforcement of PEGDA or PVP also exhibited excellent dimensional stability and film homogeneity. These films, while appearing as transparent as MEEP-(LiAlCl$_4$)$_n$, were softer than the latter. Prolonged UV irradiation for 20 min or more, instead of the typical 5 min, led these polymer composite films to acquire a yellow coloration.

Mechanically stable electrolyte films could also be cast from solutions of a mixture of MEEP and PEO or MEEP and PPO in acetonitrile containing an appropriate Li salt. It appears that when the electrolyte matrix is interspersed with an appropriate amount of PEO or PPO, a dimensionally stable film can be prepared irrespective of the salt. We have demonstrated this with LiBF$_4$, LiClO$_4$, LiAsF$_6$, LiCF$_3$SO$_3$, LiAlCl$_4$, and LiN(SO$_2$CF$_3$)$_2$. An important observation was that when the mixture contained MEEP and PEO, a homogeneous electrolyte could be prepared only if the amount of MEEP was ≤70 wt% of the polymer mixture. For higher MEEP/PEO weight ratios, the films appeared heterogeneous with isolated regions of PEO and MEEP. Mixtures of MEEP and PPO, on the other hand, formed homogeneous solid solutions at all proportions, and mechanically strong MEEP/PPO-(LiX)$_n$ electrolytes could be prepared if the amount of PPO was at least 20 wt% of the polymer mixture. Some of our results on MEEP/PEO-(LiX)$_n$ and MEEP/PPO-(LiX)$_n$ have already been reported.[8,9]

Structure of MEEP-Based Electrolytes. We may first recall that polymer electrolytes are complexes of Li salts with polymers having electron-donor atoms such as O or N. Lithium salts will dissolve in the polymer if the free energy for complex formation between Li$^+$ and the polymer exceeds the lattice energy of the salt. The ionic conductivity of the resulting electrolyte will depend on a number of factors including the permittivity of the medium and the concentration of the ions and their mobility. The ionic conductivity of polymer electrolytes is believed to be through the disordered (amorphous) domains of the polymer matrix and is assisted by the large-amplitude segmental motion of the polymer backbone. The structures of PEO-(LiX)$_n$ complexes and their ionic conductivity mechanisms have been discussed.[13,14] A review of polymer electrolytes based on mixed polymers and interpenetrating polymer network is given in ref 14, particularly Chapter 6.

X-ray analysis revealed that all the MEEP-based electrolytes, except the MEEP/PEO-(LiX)$_n$ composites where LiX = LiClO$_4$ and LiBF$_4$, lacked Bragg peaks characteristic of crystalline materials. These observations are also consistent with the differential scanning calorimetric (DSC) data discussed below. X-ray patterns for several MEEP/PEO-(LiClO$_4$)$_n$ complexes are presented in Table I and are compared to the patterns for LiClO$_4$, PEO, and PEO-(LiClO$_4$)$_{0.13}$. The data for the latter electrolyte show peaks due to PEO at 2.32 and 1.93 Å along with a strong line at 3.00 Å, most probably due to a crystalline PEO-(LiClO$_4$)$_n$. Crystalline PEO-(LiClO$_4$)$_n$ complexes have been previously identified,[13] including a material with $n = \sim0.33$ melting at about 160 °C and a complex with $n = \sim0.17$ and a melting point of about 65 °C. On the basis of the Li salt to polymer ratio, the complex in our case most probably is the latter. The X-ray diffraction patterns of MEEP/PEO-(LiClO$_4$)$_{0.13}$ complexes show the principal line of PEO at 1.96 Å and of PEO-(LiClO$_4$)$_n$ at 3.02 Å. The line at 2.02 Å is common to all the MEEP/PEO mixed electrolytes, and its intensity increases with the amount of MEEP in the sample. Since MEEP-(LiClO$_4$)$_n$ itself is amorphous, we may ascribe the line at 2.02 Å to a mixed complex formed between LiClO$_4$ and MEEP and PEO. X-ray data for MEEP/PEO-(LiBF$_4$)$_n$ could also be interpreted in a similar way. Thus, the MEEP/PEO-(LiX)$_{0.13}$ mixed electrolyte films appear to

(12) Tada, H., Kawahara, H. *J. Electrochem. Soc.* **1988**, *135*, 1728.

(13) Wright, P. V. *J. Macromol. Sci.* **1989**, *A26*, 519.
(14) MacCallum, J. R., Vincent, C. A., Eds.; *Polymer Reviews*; Elsevier Applied Science: New York, 1987.

Table I. X-ray Diffraction Data for LiClO₄, PEO, and Polymer Electrolytes (d, Å)^{a,b}

LiClO₄	PEO	PEO-(LiClO₄)$_{0.13}$	MEEP/PEO-(LiClO₄)$_{0.13}$			
			40/60^c	50/50^c	60/40^c	70/30^c
		3.00$_{100}$	3.02$_{60}$	3.02$_{70}$	3.01$_{80}$	3.03$_{100}$
	2.31$_{70}$	2.32$_{40}$				
2.16$_{20}$						
			2.02$_{10}$	2.04$_{60}$	2.02$_{40}$	2.02$_{90}$
	1.92$_{100}$	1.93$_{80}$	1.96$_{100}$	1.96$_{100}$	1.96$_{100}$	1.96$_{90}$
1.82$_{100}$	1.80$_{20}$					
1.76$_{30}$	1.73$_{10}$					
1.40$_{20}$				1.60$_{10}$	1.60$_{10}$	
1.30$_{20}$						
1.24$_{20}$					1.48$_{6}$	
1.23$_{30}$						
1.09$_{10}$						

^{a}The subscripts refer to the relative intensity of the X-ray lines. ^{b}All the electrolytes were X-rayed at least 4 weeks after they were prepared. ^{c}Weight ratio of polymers in percentage.

Figure 1. Comparison of the IR spectra of PEO and PEO-(LiClO₄)$_{0.13}$.

Figure 2. IR spectra of MEEP, MEEP-(LiClO₄)$_{0.25}$, and MEEP-(LiAlCl₄)$_{0.25}$.

be a composite of the three crystalline phases of PEO, PEO-(LiX)$_n$, MEEP/PEO-(LiX)$_n$ plus amorphous MEEP and possibly an amorphous MEEP-(LiX)$_n$ complex. By analogy, a similar distribution of single and mixed polymer complexes can be visualized in the case of MEEP/PPO-(LiX)$_n$ composites. However, X-ray data indicated the latter to be amorphous.[9] It may be argued that the MEEP/PVP-(LiX)$_n$ and MEEP/PEGDA-(LiX)$_n$ are also composed of single and mixed polymer complexes of Li salts, although X-ray and DSC data were of little help in resolving this issue. Both of these complexes were amorphous to X-rays. The MEEP/PEO mixed complexes of LiN(SO₂CF₃)₂, in contrast to the electrolytes derived from the other salts, were fully amorphous. As shown later in this paper, they are among the highest conducting dimensionally stable electrolytes reported to date. It should also be noted that MEEP-(LiAlCl₄)$_n$, despite its dimensional stability, was amorphous to X-rays in the same manner as the glutinous complexes.

Infrared spectra were examined to gain further insight into the structures of the electrolytes. The IR spectra for PEO, PEO-(LiClO₄)$_{0.13}$, MEEP, MEEP-(LiClO₄)$_{0.25}$, and MEEP-(LiAlCl₄)$_{0.25}$ are presented in Figures 1 and 2. The 1500–500-cm⁻¹ spectral region was the most informative. The infrared spectra of PEO and a number of PEO-(LiX)$_n$ complexes have been discussed by Papke et al.,[15] although their paper did not include LiClO₄ complexes. Also, Papke et al.'s PEO had a molecular weight of 6 × 10⁵ as opposed to 5 × 10⁶ for the material in this work and they primarily dealt with PEO-(LiX)$_{0.25}$ while the focus here is on PEO-(LiX)$_{0.125}$. The infrared spectrum of our PEO is

(15) Papke, B. L.; Ratner, M. A.; Shriver, D. F. *J. Electrochem. Soc.* **1982**, *129*, 1434.

identical with that reported in ref 15. However, in several respects our spectrum of PEO-(LiClO₄)$_{0.125}$ differs from that of PEO-(LiBF₄)$_{0.25}$ and other complexes given in ref 15. Relative to the spectrum of PEO, our spectrum of PEO-(LiClO₄)$_{0.125}$ in Figure 1 reveals clearly discernible new peaks at 1590, 1371, 1320, 920, 827, 815, 625, and 572 (doublet) cm⁻¹. The broad, apparently triplet, peak around 1110 cm⁻¹ in PEO has become broader in PEO-(LiClO₄)$_{0.125}$. The 625-cm⁻¹ peak in the complex is due to absorptions of the ClO₄⁻ anion, and the broadening of the C–O–C linkage vibration around 1110 cm⁻¹ is indicative of C–O → Li⁺ complexation. The presence of the new IR peaks in addition to the peaks for neat PEO in our complex is consistent with a material containing both uncomplexed PEO and the PEO-(LiClO₄)$_n$ complex. A very distinct feature of the spectrum is the doublet at 572 cm⁻¹ associated with O–C–C bending in the PEO-(LiClO₄)$_{0.125}$ complex, a counterpart of the peak at 520 cm⁻¹ in neat PEO. (This vibrational assignment is according to ref 15). It appears that Papke et al. did not observe a clear distinction between PEO and PEO-(LiX)$_n$ because in their complexes n was about 0.25 so that very little free PEO existed.

The IR spectra of MEEP, MEEP-(LiAlCl₄)$_{0.25}$, and MEEP-(LiClO₄)$_{0.25}$, depicted in Figure 2, are characterized by a number of broad absorption peaks in the 750–1500-cm⁻¹ region from which no significant information relevant to the structure of the complex could be gained. In these materials the P=N and C–O–C stretching vibrations are found at about 1250 and 1100 cm⁻¹, respectively. The Cl–O stretching vibrational peak in the LiClO₄ complex is found at 623 cm⁻¹. This peak was also present in the MEEP/PEO-(LiClO₄)$_{0.13}$ complexes. The IR spectrum of MEEP-(LiAlCl₄)$_{0.25}$ shows features similar to those found

Figure 3. DSC traces of MEEP–(LiAlCl$_4$)$_n$ complexes.

Figure 4. DSC traces of PEO–(LiClO$_4$)$_{0.125}$ and 55 MEEP/45 PEO–(LiClO$_4$)$_{0.13}$.

Figure 5. Conductivities of the LiBF$_4$ complexes of MEEP, PEO, PPO, and a MEEP/PPO mixture.

in MEEP–(LiClO$_4$)$_{0.25}$. A peak due to AlCl$_4^-$ is not observed since its absorption occurs around 480 cm^{-1}.[16]

Differential scanning calorimetric (DSC) traces of MEEP–(LiX)$_n$, where LiX = LiClO$_4$, LiBF$_4$, and LiSO$_3$C-F$_3$, were all without any peaks in the 25–200 °C range. The DSC traces of three MEEP–(LiAlCl$_4$)$_n$ films are presented in Figure 3. The broad endotherm extending from around 60 to 140 °C may correspond either to the ill-defined melting of a partially crystalline phase or to the removal of solvents that remain in the film after being cast from solutions.

The DSC data for 55 MEEP/45 PEO–(LiClO$_4$)$_{0.13}$ and PEO–(LiClO$_4$)$_{0.13}$ are presented in Figure 4. The latter shows two closely lying peaks at 58 and 65 °C, probably associated with the melting of crystalline PEO and a PEO–(LiClO$_4$)$_n$ complex. The DSC thermogram for 55 MEEP/45 PEO–(LiX)$_n$ appears to contain melting point transitions at 53 and 63 °C with possibly a third, lower melting, peak at about 44 °C. The latter may correspond to the mixed complex indicated by the X-ray diffraction pattern. It should be noted that when the mole fraction of the salt n was 0.18 and 0.25, higher melting complexes were indicated by the DSC data for MEEP/PEO mixed electrolytes containing LiBF$_4$ and LiClO$_4$.[8] The DSC thermograms for 87 MEEP/13 PEGDA–(LiClO$_4$)$_{0.25}$ and 87 MEEP/13 PVP–(LiClO$_4$)$_{0.25}$ were also without endothermic peaks in the 25–200 °C range, and they indicated that the former is stable up to at least 200 °C whereas the latter may decompose at about 190 °C.

The structural data we have obtained suggest that generally speaking the crystalline–amorphous morphology

of the mixed polymer electrolytes is related to that of the individual electrolytes of which they are composed. LiN-(SO$_2$CF$_3$)$_2$ complexes are an exception. The large imide anion appears to discourage precipitation of crystalline complexes so that the related electrolytes may remain as amorphous phases. The improved dimensional stability of the composite electrolytes compared to MEEP–(LiX)$_n$ is attributable to the fact that the mechanically strong, second polymer phase dispersed into the film matrix reinforces its overall mechanical strength. The Li$^+$ seems to complex with MEEP as well as the second polymer phase in the mixed electrolyte, which is in keeping with the fact that the electron-donating heteroatom in both MEEP and the second polymer is oxygen bonded to carbon. The structural factors responsible for the unusual dimensional stability of MEEP–(LiAlCl$_4$)$_n$ are presently unknown. It is possible that the AlCl$_4^-$ anions serve as cross-links between the polymer chains, probably involving interactions with the P=N bonds. This, however, remains to be confirmed.

Ionic Conductivity and Transport. The specific conductivity versus temperature data presented in Figure 5 illustrate how the conductivity of a MEEP/poly(olefin oxide)–(LiX)$_n$ mixed polymer electrolyte relates to that of electrolytes derived from the individual polymers. The conductivity versus $1/T$ behavior of MEEP–(LiBF$_4$)$_{0.25}$ and PPO–(LiBF$_4$)$_{0.13}$ is indicative of these polymers being fully amorphous. That is, the conductivity increases in a monotonic fashion with increasing temperature, which as previously discussed[14] is in accordance with the Vogel–Tamann–Fulcher relationship $\sigma = AT^{-1/2} \exp(-E_a/R(T - T_0))$ for a predominantly amorphous polymer. There are two important features in the σ versus $1/T$ curves for PEO–(LiBF$_4$)$_{0.125}$ and MEEP/PEO–(LiBF$_4$)$_{0.125}$: (i) the cooling and heating curves show hysteresis; (ii) two distinct temperature regions appear in which the slopes of the curves that correspond to the activation energy for conduction have different values; below 60 °C the slope is much steeper than above 60 °C.

It is well-known that the abrupt increase in conductivity at about 60 °C in PEO-based electrolytes is due to the melting of crystalline PEO and the consequent formation of a uniformly plastic electrolyte phase. The term "plastic phase" is preferred here to indicate the more fluid nature of this phase, as opposed to the term "amorphous phase", which does not necessarily imply increased fluidity. Indeed, PPO–(LiBF$_4$)$_{0.13}$ is fully amorphous over same temperature range given in Figure 5, yet its conductivity at 75 °C is significantly lower than that of the others. This
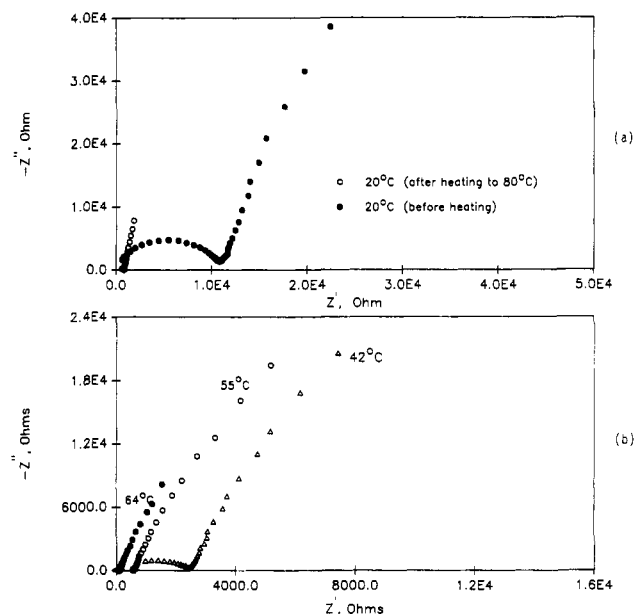
(16) Doorenbos, H. E.; Evans, J. C.; Kagel, R. O. *J. Phys. Chem.* **1970**, *74*, 3385.

Figure 6. (a) Room-temperature complex impedance spectra for the electrolyte 55 MEEP/45 PEO-$(LiBF_4)_{0.13}$, recorded between stainless steel blocking electrodes as fresh and after heating to 80 °C followed by cooling to room temperature. (b) Fresh electrolyte recorded at 45, 55, and 65 °C.
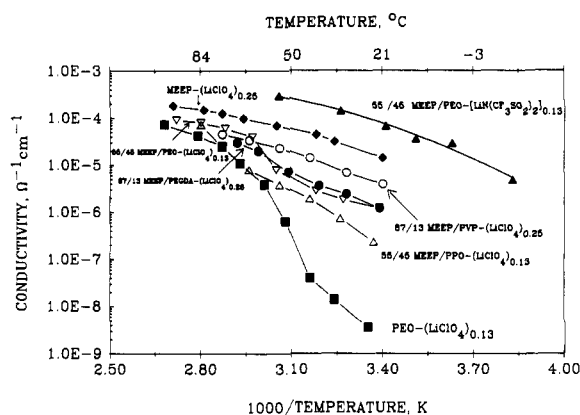

Figure 7. Comparison of the conductivities of several MEEP-based electrolytes.

Table II. Conductivities of a Number of MEEP-Based Electrolytes at 25 and 50 °C

polym electrolytes	conductivity, Ω^{-1} cm^{-1}	
	25 °C	50 °C
MEEP-$(LiClO_4)_{0.25}$	1.7×10^{-5}	5.0×10^{-5}
55 wt % MEEP/45 wt % PEO-$(LiClO_4)_{0.13}$	1.3×10^{-6}	9.0×10^{-6}
55 wt % MEEP/45 wt % PPO-$(LiClO_4)_{0.13}$	9.0×10^{-8}	3.5×10^{-6}
MEEP-$LiN(CF_3SO_2)_2$	6.5×10^{-5}	1.6×10^{-4}
55 wt % MEEP/45 wt % PEO-$[LiN(CF_3SO_2)_2]_{0.13}$	6.7×10^{-5}	1.2×10^{-4}
87 wt % MEEP/13 wt % PVP-$(LiClO_4)_{0.13}$	4.0×10^{-6}	2.3×10^{-5}
87 wt % MEEP/13 wt % PEGDA-$(LiClO_4)_{0.13}$	1.2×10^{-6}	7.2×10^{-6}
MEEP-$(LiAlCl_4)_{0.13}$	1.2×10^{-5}	4.0×10^{-5}

is most probably due to a relatively lower amount of fluidity in this electrolyte. The usual argument based on poorer complexation of Li$^+$ by PPO does not appear to be fully satisfactory in view of the rather similar conductivity of both PEO and PPO complexes below 60 °C. It is also interesting that above 60 °C, the conductivities of $LiBF_4$ complexes of PEO, PEO/MEEP mixture, and MEEP are all rather similar. At this temperature, the three electrolytes appear to reach a rather similar state of "plasticity" whereby the large amplitude segmental motion of the polymer backbone that assists the conductivity of the ions becomes appreciable. As with PEO-$(LiX)_n$, MEEP/PEO-$(LiX)_n$ electrolytes also exhibit hysteresis in their σ vs $1/T$ plots associated with heating and cooling. During cooling, the shape of the plot was altered significantly with almost a complete elimination of the knee between 50 and 60 °C. The heated electrolyte was found to maintain the high conductivity for an extended period of time at room temperature. The original conductivity–temperature relation is recovered after 1 month at room temperature.

The activation energy for conduction in MEEP/PEO-$(LiBF_4)_n$ was determined as a function of the ratio of the two polymers and the salt concentration.[8] For the 55/45 polymer weight ratio, the activation energy below 60 °C was insensitive to salt concentrations corresponding to n between 0.016 and 0.18. However, activation energy increased substantially when the amount of MEEP decreased from 70 to 50 wt%. This behavior is consistent with higher plasticity for electrolytes having higher MEEP contents. Above 60 °C, correlations between activation energy and electrolyte composition were not straightforward.

Figure 6 displays complex impedance spectra for 55 MEEP/45 PEO-$(LiBF3)_{0.13}$ at different temperatures. The ac frequency range was between 6 Hz and 100 kHz. For fresh electrolytes at room temperature, the Cole–Cole spectrum represented a semicircle with a spur at low frequencies. This represents an equivalent circuit in which the electrode capacitance is in series with a parallel combination of electrolyte resistance and its capacitance. With increasing temperature the semicircle gave way to the spur,

and at a temperature above the melting point of PEO only a straight line usually remained. At these temperatures, the capacitative component of the electrolyte appears to be negligible up to a frequency of 100 kHz. The high plasticity induced at temperatures above the melting point of PEO appears to decrease the dielectric relaxation times of the electrolyte so that in our frequency range of impedance measurement the electrolyte capacitance becomes negligible. In fact, as shown in Figure 6a, the electrolyte heated once to 80 °C and then cooled to 20 °C shows an impedance spectrum indicative of a highly plastic electrolyte. Similarly, MEEP-$(LiX)_n$ at room temperature showed impedance spectra with profiles resembling that of 55 MEEP/45 PEO-$(LiBF_4)_{0.13}$ at 64 °C.

It can be seen from the data in Figure 7 that the conductivities of the other mixed electrolytes MEEP/PEO-$(LiX)_n$, MEEP/PVP-$(LiX)_n$, and MEEP/PEGDA-$(LiX)_n$ are also very high at room temperature, being only about an order of magnitude lower than that of MEEP-$(LiX)_n$. Conductivities at 25 and 50 °C for a group of electrolytes are listed in Table II. The data illustrate some interesting effects of Li salt on conductivity. The dimensionally stable films of 55 MEEP/45 PEO-$[LiN(SO_2CF_3)_2]_{0.13}$ exhibited a room-temperature conductivity higher than that of all the MEEP-$(LiX)_n$ complexes except MEEP-$[LiN(SO_2CF_3)_2]_{0.13}$, whose conductivity is identical with that of the MEEP/PEO mixed electrolyte containing the imide salt. The complex impedance spectrum of 55 MEEP/45 PEO-$(LiN(SO_2CF_3)_2)_{0.13}$ had a profile similar to that shown in Figure 6b, obtained at 64 °C.

The conductivities of $LiAlCl_4$ complexes of MEEP are presented in Figure 8 as plots of σ vs $1/T$. Despite its good mechanical strength, the conductivity of
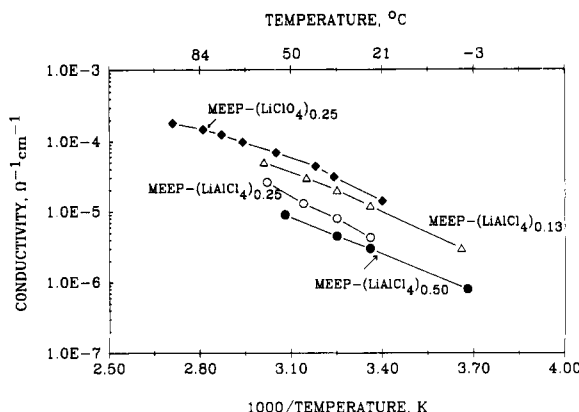
Figure 8. Conductivities of MEEP-(LiAlCl$_4$)$_n$ complexes.

MEEP-(LiAlCl$_4$)$_{0.13}$ at room temperature is almost the same as that of MEEP-(LiClO$_4$)$_{0.25}$. The corresponding impedance spectra also resembled the 64 °C spectrum in Figure 6b. Apparently MEEP-(LiAlCl$_4$)$_n$ retain a high degree of plasticity even at room temperature. At higher LiAlCl$_4$ concentrations the conductivity decreases perhaps due to increased ion pairing.

The results we have obtained suggest that the dimensionally stable electrolytes derived from LiN(SO$_2$CF$_3$)$_2$ and LiAlCl$_4$ retain good plasticity even in a solid matrix to produce high conductivity at room temperature in the corresponding electrolyte films. Evidently, polymer electrolytes having an ability to retain a high degree of plasticity or microfluid domains in a solid matrix are the ones expected to be highly ionically conductive while being dimensionally stable. Indeed, the higher room-temperature conductivity of the MEEP/PVP-(LiClO$_4$)$_{0.25}$ composite electrolyte compared to its PEO or PPO composite counterpart may be ascribed to a predominantly plastic phase of MEEP-(LiClO$_4$)$_n$ contained in a solid matrix in which PVP acts primarily as a matrix reinforcement to impart mechanical strength to the electrolyte.

The results presented above demonstrate that several convenient methods are now available for the preparation of dimensionally stable, MEEP-based, free-standing electrolytes whose conductivities are comparable to those of MEEP-(LiBF$_4$)$_{0.25}$ and MEEP-(LiClO$_4$)$_{0.25}$, which have poor mechanical stability. The good mechanical strength of the LiAlCl$_4$ complexes is interesting, especially in view of the fact that they did not exhibit any significant amount of crystallinity. It may be noted here that the behavior of MEEP/PEO mixed polymer electrolytes containing LiAlCl$_4$ we reported previously[8] was somewhat peculiar. For example, the conductivity of MEEP/PEO-(LiX)$_{0.13}$ electrolytes decreased in the order LiBF$_4$ $\simeq$ LiClO$_4$ > LiCF$_3$SO$_3$ > LiAsF$_6$ > LiAlCl$_4$. The LiAlCl$_4$-containing films were all characterized by more rigidity than the others, probably indicating the unusual interaction of the AlCl$_4^-$ anion with the polymer chain.

The Li$^+$ transport number (t_+) of some selected MEEP-based mixed-polymer electrolytes was determined by using the potentiostatic polarization technique.[11] Table III lists the values for electrolytes having different polymer compositions and two different Li salts, namely, LiClO$_4$ and LiBF$_4$. As can be seen in this table, transport numbers around 0.40 were obtained for Li$^+$ in these electrolytes. The reason for the somewhat higher transport number of the LiBF$_4$ complex of MEEP/PEO is not clear at this time. Previously,[14] t_+ of 0.32 and 0.17, respectively, were obtained for MEEP-(LiCF$_3$SO$_3$)$_{0.17}$ and MEEP-(LiBF$_4$)$_{0.17}$ electrolytes. It is worth noting also that the transport numbers in PEO-(LiX)$_n$[16,17] electrolytes ranged between 0.4 and 0.5.

Table III. Transport Numbers for Li$^+$ in Some MEEP-Based Electrolytes

cell	electrolyte	t_+
1	87/13 MEEP/PEGDA-(LiClO$_4$)$_{0.13}$	0.40
2	70/30 MEEP/PEO-(LiClO$_4$)$_{0.13}$	0.44
3	70/30 MEEP/PEO-(LiClO$_4$)$_{0.13}$	0.36
4	70/30 MEEP/PEO-(LiBF$_4$)$_{0.13}$	0.40
5	55/45 MEEP/PEO-(LiBF$_4$)$_{0.13}$	0.39
6	55/45 MEEP/PEO-(LiBF$_4$)$_{0.13}$	0.34
7	55/45 MEEP/PPO-(LiBF$_4$)$_{0.13}$	0.52
8	55/45 MEEP/PPO-(LiClO$_4$)$_{0.13}$	0.40

Since the mobile cations in polymer electrolytes are triple and/or quadruple ions, the t_+ reported here does not strictly represent transport number for Li$^+$. It is more accurately described as the dc conductivity which transports Li ions from the negative to the positive electrode.

The higher the ionic conductivity for an electrolyte, the lower the resistive polarization (iR drop) during discharge of a Li cell utilizing the electrolyte. On the other hand, a transport number of less than 1 for Li$^+$ implies migration of the anion to the Li electrode during cell discharge until a steady-state discharge current is reached. This results in the accumulation of Li salt at the Li–electrolyte interface and possible interfacial polarization of the Li electrode. The effect of Li$^+$ transport number on the steady-state limiting current of a Li cell, e.g., a Li/TiS$_2$ cell, can be described in terms of the relationship in eq 1.[17]

$$I_1 = \frac{2nFD_{Li}^+C_b}{d(1 - t_+)} \qquad (1)$$

In this equation, D_{Li}^+, C_b, and t_+ are the diffusion coefficient, the bulk concentration, and transport number of Li$^+$, and d is the interelectrode spacing, which includes the thickness of the porous cathode. An optimized solid-state cell will utilize a 0.5-mm-thick electrolyte film and a 0.1-mm-thick cathode. The concentration of Li$^+$ in the 55 MEEP/45 PEO-(LiClO$_4$)$_{0.13}$ electrolyte is 1.8 mol/L. Assuming a diffusion coefficient of 10^{-7} cm^2/s for Li$^+$ at 70 °C and a Li$^+$ transport number of 0.4, the steady-state limiting current can be calculated to be 0.6 mA/cm^2. Equation 1 shows that the limiting current can be increased by adjusting a variety of parameters including a higher salt concentration, smaller interelectrode distance, and higher diffusion coefficient and transport number for Li$^+$.

Electrochemical Stability. Cyclic voltammetric studies at stainless steel or gold working electrodes were carried out to assess the electrochemical stability domain of the MEEP-based mixed polymer electrolytes. Ideally, a polymer electrolyte should exhibit a stability domain between 0.0 and 4.0 V, the potential region where the electrochemical reactions of the Li negative and the positive electrodes occur. Figure 9a shows the voltammetric scan of a 55 wt% MEEP:45 wt% PEO-(LiClO$_4$)$_{0.13}$ at a scan rate of 2 mV/s at 75 °C. The electrode was stainless steel. The electrode was swept first cathodically from the open-circuit potential of 2.8 to −1 V, followed by an anodic sweep up to 5 V. The potentials reported here are with respect to the Li$^+$/Li electrode and are without iR compensation.

The first small rise in reduction current took place at about 1.4 V, followed by another small cathodic current peak beginning at 0.7 V. Both of these peaks appear to be associated with corresponding anodic peaks of much smaller magnitude at about 2.2 and 1.3 V, respectively. We

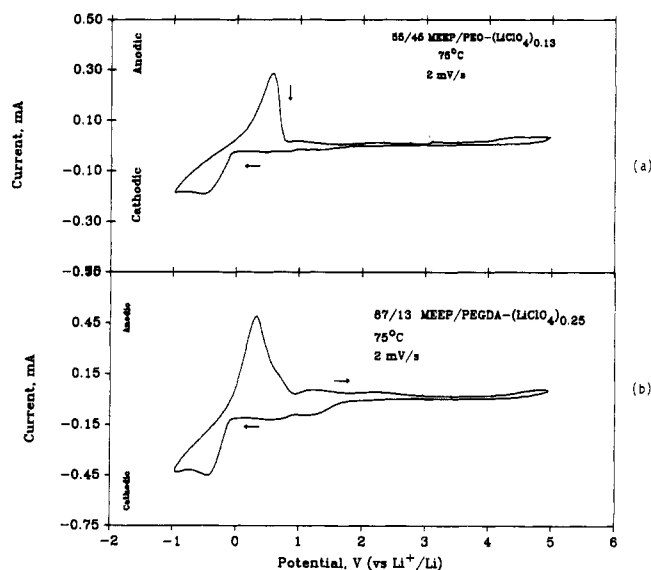(17) Atlung, S.; West, K.; Jacobsen, T. *J. Electrochem. Soc.* **1979**, *126*, 1311.

Figure 9. Cyclic voltammograms of (a) 55 MEEP/45 PEO-(LiClO$_4$)$_{0.13}$ and (b) 87 MEEP/13 PEGDA-(LiClO$_4$)$_{0.13}$ on a stainless steel electrode at 75 °C. Scan rate = 2 mV/s.

have observed peaks at potentials very close to these also in the cyclic voltammograms of MEEP/PPO-LiClO$_4$,[9] poly(tetrahydrofuran)-LiClO$_4$,[18] and poly(1,3-dioxolane)-LClO$_4$ electrolytes.[18] The common species in these electrolytes is LiClO$_4$, suggesting that these peaks may be associated with the reduction and oxidation of LiClO$_4$. It appears that the polymer itself undergoes little reduction at these low potentials. The sharp rise in cathodic current beginning at –0.2 V is due to the reduction of Li$^+$ and the deposition (plating) of the resulting Li on the stainless electrode, eq 2. The anodic peak centered

$$Li^+ + e^- \rightleftharpoons Li \qquad (2)$$

around 1.5 V can be ascribed to the stripping (oxidation) of the Li. Comparison of the quantities of charge involved in Li plating and stripping reveals that the processes are fully chemically reversible. A very small anodic peak around 4.5 V was observed on further scanning the electrode up to a potential of 5.0 V. As shown in Figure 9b, voltammograms similar to these were also obtained with the MEEP/PEGDA-LiClO$_4$ electrolyte. The effect of Li salt on electrolyte stability was investigated with the cyclic voltammogram of 55 MEEP/45 PEO-(LiBF$_4$)$_{0.13}$ (Figure 10). The Li stripping process was followed by another closely lying peak that assumed a distinct shape on continued cycling (Figure 10b). Despite the two steps associated with the stripping process, Li cycling appeared to be fully chemically reversible. We can explain the two steps in the Li stripping process as follows. Li being plated on the stainless steel electrode is in two different environments: a first layer adjacent to the stainless steel electrode and strongly adsorbed to it, and a second fraction residing on the first layer of Li. Consequently, the second fraction of Li is stripped at a potential closer to the Li$^+$/Li potential than the first fraction, which is stripped at a slightly more positive potential.

Figure 11 presents the cyclic voltammogram of 55 MEEP/45 PEO-(LiClO$_4$)$_{0.13}$ electrolyte at a gold working electrode. Again, as in Figure 9, there are two very small peaks around 1.5 and 0.9 V prior to the main reduction peak beginning at around 0.2 V. The oxidation peak
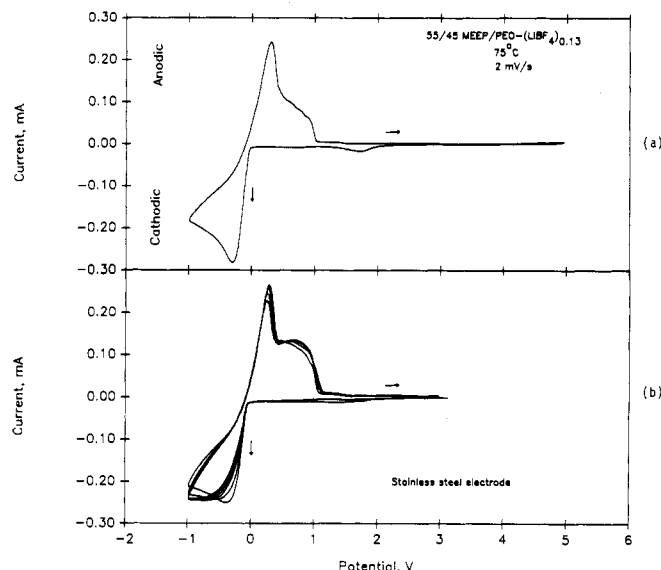
(18) Abraham, K. M.; Alamgir, M.; Moulton, R. D. *Electrochim. Acta*, in press.

Figure 10. Cyclic voltammogram of 55 MEEP/45 PEO-(LiBF$_4$)$_{0.13}$ on a stainless steel electrode at 75 °C. Scan rate = 2 mV/s; (a) first scan, (b) several scans beginning with the second scan.
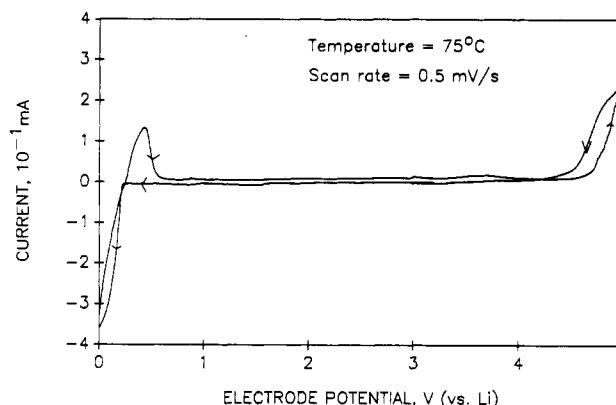

Figure 11. Cyclic voltammogram of 55 MEEP/45 PEO-(LiClO$_4$)$_{0.13}$ at a gold electrode at 75 °C. Scan rate = 0.5 mV/s.

corresponding to the reduction at 0.2 V was observed around 0.5 V, and the reduction and oxidation processes appeared to be chemically reversible. Unlike on a stainless steel electrode where the plating of Li occurred, as expected, at a potential negative of Li$^+$/Li, Li plating on Au takes place at a potential positive of Li$^+$/Li. This behavior is similar to that found when the electrode is Al or other metals that can alloy with Li.[19] Indeed, Li and Au forms an alloy of the composition Li$_3$Au.[19] The alloying of Li with and dealloying of Li from Au at 75 °C exhibits good chemical reversibility. On further scanning the electrode anodically, an appreciable current began to appear at around 4.7 V. On a return sweep, there was a crossover of the oxidation and the reduction peaks, presumably due to electrode passivation from adsorption of electroactive species on the electrode. The gold electrode, unlike stainless steel, appeared black after excursion to the Li plating potential, supporting the formation of an alloy of Li and Au.

The cyclic voltammogram of the 55 MEEP/45 PEO-(LiBF$_4$)$_{0.07}$ electrolyte on a glassy carbon electrode

(19) Dey, A. N. *J. Electrochem. Soc.* 1971, *118*, 1547.
(20) Vassort, G.; Gauthier, M.; Harvey, P. E.; Brochu, F.; Armand, M. B. *Proceedings of the Symposium on Lithium Batteries*; Fall Meeting of the Electrochemical Society, Honolulu, HI, 1987; PV88-6, pp 780–793.

MEEP-Based Polymer Electrolytes

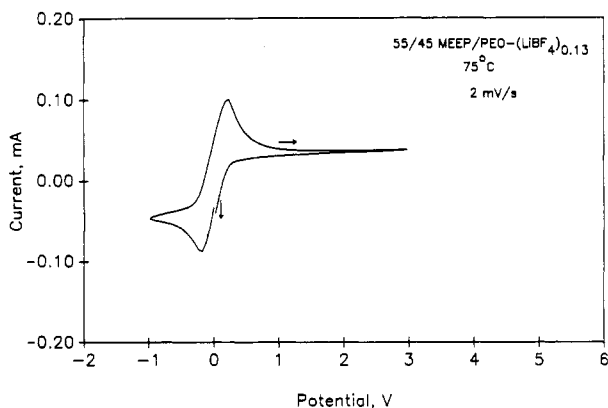*Chem. Mater., Vol. 3, No. 2, 1991* 347

Figure 12. Cyclic voltammogram of 55 MEEP/45 PEO-(LiBF$_4$)$_{0.13}$ on a Li electrode at 70 °C. Scan rate = 2 mV/s.
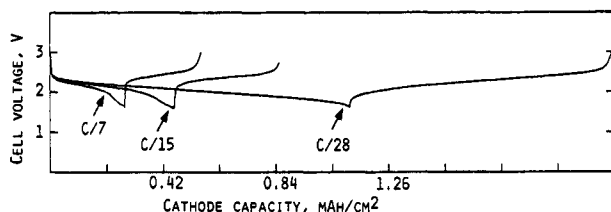

Figure 13. Capacity–rate behavior of a Li/TiS$_2$ cell using fiberglass matrix supported MEEP-(LiClO$_4$)$_{0.25}$ electrolyte at 50 °C. The discharge rate is indicated on each curve.

Figure 14. Long-term cycling behavior of a Li/TiS$_2$ cell using fiberglass matrix supported MEEP-(LiClO$_4$)$_{0.25}$ electrolyte at 50 °C. Current, i_d = 0.2 mA/cm^2; i_c = 0.05 mA/cm^2; voltage limits = 1.6–3.0 V.

Figure 15. Effect of overcharge on the cycling of a Li/TiS$_2$ cell utilizing MEEP-(LiClO$_4$)$_{0.25}$. Current is the same as in Figure 14. The numbers on the curves indicate cycles.

showed a reduction peak at 2.1 V, followed by two small reduction peaks at 1.35 and 0.45 V. The current involved in these reduction processes on carbon was higher than that observed on the metal electrodes and may be indicative of a catalytic effect of carbon. A peak at 0.45 V, probably corresponding to the intercalation of Li into C, was also observed. The latter process is typically observed in the voltammograms of carbon in nonaqueous electrolytic solutions containing Li salts. The practical relevance of the electrochemistry of polymer electrolytes on a carbon surface lies in the fact that high-surface-area carbon is used as an additive in the cathode structure of Li batteries to enhance electronic conductivity of the electrode. Any redox processes involving the electrolyte on the cathode can affect battery performance. The anodic stability of the electrolytes on carbon exceeded 4.25 V versus Li$^+$/Li.

The cycling of the 55 MEEP/45 PEO-(LiBF$_4$)$_{0.13}$ electrolyte on a Li metal substrate is illustrated in Figure 12. The plating and stripping of Li are the only electrochemical processes occurring here. Practically no reduction of the electrolyte is observed. This is extremely significant since unwanted side reactions of the electrolyte that can interfere with Li plating and stripping will be of little concern here.

Solid-State Li/TiS$_2$ Cells. Li/TiS$_2$ cells utilizing the dimensionally stabilized MEEP electrolytes were fabricated and galvanostatically discharged and charged (cycled) at several temperatures including 20, 50, and 75 °C. Since MEEP-(LiX)$_n$ itself is dimensionally unstable, it was immobilized by incorporation into the pores of a fiberglass filter paper.[4] This enabled comparisons of the rate capabilities of neat MEEP electrolytes with MEEP-based composite electrolytes.

The open-circuit potentials of freshly prepared cells were between 2.8 and 2.9 V, which on heating to 50 °C declined slightly to values between 2.6 and 2.8 V. Figure 13 shows typical constant current charge–discharge curves of a Li/TiS$_2$ cell using MEEP-(LiClO$_4$)$_{0.25}$ electrolyte supported in a fiberglass separator paper. The cells were discharged to a voltage limit of 1.6 V and charged to 3.0
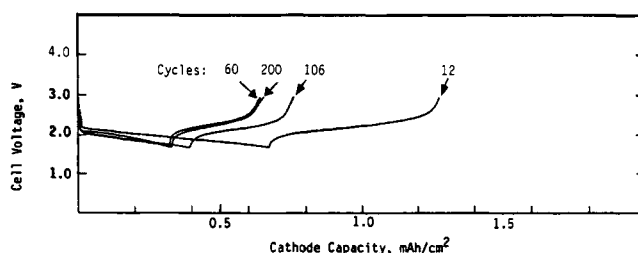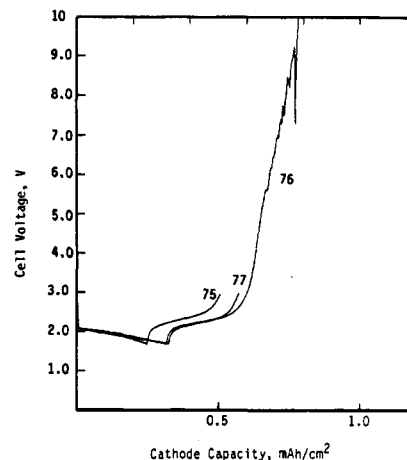
V. The data encompass three different rates at 50 °C. The current densities were 0.05, 0.1, and 0.2 mA/cm^2 at the C/28, C/15, and C/7 rates. The cell delivered the capacities of 1.10, 0.45, and 0.28 mAh/cm^2, respectively, at these rates. Increasing the discharge temperature from 50 to 75 °C more than doubled the capacity of the cell. The mid-discharge voltage was 2.1 V, while the average charging potential was 2.5 V. The Coulombic efficiency during the cycling was between 90 and 100%.

Figure 14 shows the long-term cycling performance of a second Li/TiS$_2$ cell using MEEP-(LiClO$_4$)$_{0.25}$ supported on a fiberglass paper matrix. The cell was cycled more than 200 times. The continuous decrease in capacity with cycling is somewhat typical of unoptimized laboratory cells in which the capacity loss is associated with several factors including cathode structural problems, inefficiencies in the recharging of the anode and cathode, and any number of mechanical reasons. However, the present data clearly show that the MEEP-based electrolytes are chemically and electrochemically stable in contact with Li and can be fabricated into long cycle life secondary Li batteries.

A knowledge of the overcharge and overdischarge behavior of a secondary Li cell, that is, discharge and charge into potential regions beyond where the normal electric current producing redox chemistry of the cell occurs, is important since such a condition could be encountered in the normal operation of a battery. Undesirable electrochemical reactions during overdischarge and overcharge can be detrimental to the stability of the cell. Figure 15 depicts that the cell can function normally even after a considerable extent of overcharge. In fact, following the overcharge that occurred inadvertently at the 76th cycle due to the malfunction of the cycling equipment, the cell had been discharged down to 0.0 V before being charged back in the 77th cycle. The overdischarge, as well as the
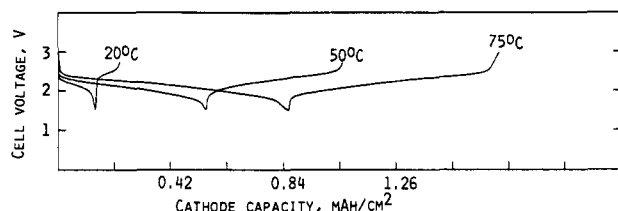
Figure 16. Constant current discharges of a Li/TiS$_2$ cell using 87 MEEP/13 PVP–(LiClO$_4$)$_{0.25}$ electrolyte at C/20 and different temperatures. i_d = 0.08 mA/cm^2; i_c = 0.04 mA/cm^2; voltage limits = 1.6–3.0 V.

overcharge, did not have a deleterious effect on subsequent cell performance.

The performance of a Li/TiS$_2$ cell using a mixed polymer electrolyte is illustrated with the MEEP–PVP–(LiClO$_4$)$_{0.25}$ electrolyte, at three different temperatures and 0.05 mA/cm^2 (C/20) (Figure 16). At room temperature the cell delivered about 17% (0.14 mAh/cm^2) of its theoretical cathode capacity of 0.88 mAh/cm^2. At 75 °C, the cathode utilization was 100%. The charging efficiency at room temperature was 85%, and at the higher temperature it was 100%, indicating slower recharge kinetics at low temperatures. The rate capability of the cell containing MEEP/PVP–(LiClO$_4$)$_{0.25}$ was very much similar to that of the cell described above utilizing MEEP–(LiClO$_4$)$_{0.25}$.

Cells utilizing MEEP/PEO–(LiClO$_4$)$_{0.13}$ composite electrolytes exhibited rate capabilities inferior to those described above. For example, a Li/TiS$_2$ cell utilizing 70 wt% MEEP:30 wt% PEO–(LiClO$_4$)$_{0.12}$ could not be discharged at room temperature at a practical rate such as C/20 or C/40. However, when it was discharged at 65 °C, about 86% of the theoretical cathode capacity, i.e., 1.2

mAh/cm^2 was obtained at the C/40 rate, while at 50 °C the utilization was 0.96 mAh/cm^2. The Coulombic efficiency during cycling was close to 100%.

Conclusions

Several relatively simple methods have been developed to prepare dimensionally stable MEEP-based electrolytes. Pure MEEP when complexed with LiAlCl$_4$ forms dimensionally stable, free-standing thin films. This contrasts the behavior of MEEP complexes we have prepared with many other commonly used Li salts. Additional methods of dimensional stabilization include blending MEEP–(LiX)$_n$ with a poly(olefin oxide) such as PEO or PPO, or forming composites with photopolymers such as PEGDA and PVP. Some of these electrolytes exhibited conductivities close to those of the dimensionally unstable MEEP–(LiX)$_n$, indicating that they retain a high degree of plasticity or domains of microfluidity. Transport numbers ranging between 0.4 and 0.5 have been determined for Li$^+$ in these electrolytes, which are very similar to that obtained in other Li$^+$–conductive polymer electrolytes. The dimensionally stabilized MEEP-based electrolytes have demonstrated good electrochemical stability on a number of metal substrates including Li. The long-term cycling capability of Li/TiS$_2$ secondary solid-state cells fabricated with these electrolytes indicate that they are useful for low-to-moderate rate applications at ambient temperature.

Registry No. PEO, 25322-68-3; PPO, 25322-69-4; PVP, 9003-39-8; PEGDA, 28158-16-9; LiBF$_4$, 14283-07-9; LiClO$_4$, 7791-03-9; LiAsF$_6$, 29935-35-1; LiCF$_3$SO$_3$, 33454-82-9; LiAlCl$_4$, 14024-11-4; LiN(SO$_2$CF$_3$)$_2$, 90076-65-6.

New Poly(carbosilane) Models. 4. Derivatization of Linear Poly[(methylchlorosilylene)methylene]: Application to the Synthesis of Functional Poly(carbosilanes) Possessing a Poly[(methylsilylene)methylene] Backbone

E. Bacqué, J.-P. Pillot,* M. Birot, J. Dunoguès,* and P. Lapouyade

Laboratoire de Chimie Organique et Organométallique (URA 35, CNRS), Université Bordeaux I, 351, Cours de la Libération, F-33405 Talence Cédex, France

E. Bouillon and R. Pailler

Laboratoire des Composites Thermostructuraux, UM 47, CNRS-SEP-UB1, Europarc 3, Avenue Léonard de Vinci, F-33610 Pessac, France

To study the mechanisms of pyrolysis of poly(carbosilanes), as well as the effect of the structure of these precursors upon properties of the resulting ceramics, novel organosilicon polymers with well-defined skeletons were prepared. Thus, linear poly(carbosilanes) formed of exactly alternate silicon atoms and methylene groups were synthesized. Owing to the presence of functional groups on silicon centers, cross-linking of these compounds was then investigated according to chemical routes, by creating disilane, disilazane, disiloxane, and hydrocarbon bridges between different poly(carbosilanic) sites. These polymers were characterized by physicochemical methods (IR, NMR, GPC, and TGA).

Introduction

The need for ceramic composites offering enhanced properties requires both continual improvement of previously reported processes and elaboration of new synthetic routes to these materials. Thus, industrial-scale production

of SiC fibers by pyrolysis of poly(carbosilanes) (PCS), according to Yajima's route, demonstrates the considerable interest in organometallic precursors.[1]

(1) Yajima, S. *Ceram. Bull.* **1983**, *62*, 893.